Design and validation of an e-textile-based wearable system for remote health monitoring

Armando Coccia[1,2], Federica Amitrano[1,2], Leandro Donisi[2,3], Giuseppe Cesarelli[2,4], Gaetano Pagano[2], Mario Cesarelli[1,2], Giovanni D'Addio[2]

[1] *Department of Information Technologies and Electrical Engineering, University of Naples 'Federico II', Naples, Italy*
[2] *Scientific Clinical Institutes Maugeri SpA SB, Pavia, Italy*
[3] *Department of Advanced Biomedical Sciences, University of Naples 'Federico II', Naples, Italy*
[4] *Department of Chemical, Materials and Production Engineering, University of Naples 'Federico II', Naples, Italy*

ABSTRACT
The paper presents a new e-textile-based system, named SWEET Shirt, for the remote monitoring of biomedical signals. The system includes a textile sensing shirt, an electronic unit for data transmission, a custom-made Android application for real-time signal visualisation and a software desktop for advanced digital signal processing. The device allows for the acquisition of electrocardiographic, bicep electromyographic and trunk acceleration signals. The sensors, electrodes, and bus structures are all integrated within the textile garment, without any discomfort for users. A wide-ranging set of algorithms for signal processing were also developed for use within the system, allowing clinicians to rapidly obtain a complete and schematic overview of a patient's clinical status. The aim of this work was to present the design and development of the device and to provide a validation analysis of the electrocardiographic measurement and digital processing. The results demonstrate that the information contained in the signals recorded by the novel system is comparable to that obtained via a standard medical device commonly used in clinical environments. Similarly encouraging results were obtained in the comparison of the variables derived from the signal processing.

1. INTRODUCTION

In recent years, wearable technologies have aroused a great deal of interest, which is expected to further continue thanks to the rapid improvements in technology. The involvement of big companies, such as Apple and Google, has fostered the focus of research activities in this field with the aim of developing and distributing wearable products ready for various applications. IDTechEx (www.idtechex.com) described the wearable technology sector as a market with great opportunities in terms of expansion, one that is expected to reach 51.6 billion USD by 2022 with a compound annual growth rate of 15.5%. In fact, billions of wearable electronic products are already being sold each year, covering various different sectors of the market, including military and defence, space exploration, health and wellness, fashion and entertainment.

Healthcare remains one of the most interesting markets, and the advantages provided by wearable technologies can potentially establish significant cost reductions for healthcare systems. The use of these technologies is increasing in clinical environments, with Holter systems used for electrocardiographic (ECG) or long-term blood pressure monitoring [1]-[2], wearable integrated systems used in polysomnographic monitoring [3], inertial measurement unit (IMU)-based systems used (attached on the patient's skin) to recognise and evaluate activity [4] or to assess postural and gait analysis [5]-[6], and a variety of other technologies being introduced. Furthermore, wearable devices

Figure 1. System architecture: 1) wearable sensing device, 2) electronic unit, 3) SWEET App, 4) cloud, 5) SWEET Lab.

for health monitoring can be easily used by the patient in the domestic environment and, when integrated within a complete communication chain, they allow for smart remote monitoring with great benefits for both caregivers and patients.

Starting from the 1990s, the process of the miniaturisation of electronic components has allowed for considering the realisation of portable devices [7]. Today, the size of electronic devices has shifted from the micro- to the nano-scale dimension, which has allowed for the realisation of minimally invasive monitoring devices that can be used by the patient in their daily activities. The focus has therefore shifted toward the concept of electronic textiles (e-textiles) or smart textiles. The term e-textile refers to a textile substrate that incorporates electronic elements that provide it with certain capabilities for sensing (biometric or external), communication (usually wireless), power transmission, and interconnection technologies while maintaining the 'wearable' capabilities much like any other garment.

The advances in e-textile technologies have led to the development of comfortable wearable garments directly integrated in internet of things (IoT) networks. Many applications have been developed exploiting this background in the field of remote monitoring, with the aim of ensuring and increasing the patient's comfort, quality of life and safety. Nevertheless, almost all the attendant projects remain within the research field and are not intended for entry into the commercial market. Here, the main barriers include the regulatory issues related to patient safety, privacy, and data management [8], [9], as well as the need for a certain degree of reliability in terms of device performance.

A detailed review of the wearable systems for health monitoring introduced up to 2010 is provided in [10], with a dedicated section on textile-based devices. The field of ECG signal monitoring is one of the fields most covered by e-textile applications. Pani et al. (2018) provided a complete survey on textile-electrode technologies for ECG monitoring [11], with all the examined prototypes exclusively used in the scientific research field with the aim of investigating the feasibility of this form of biosignal monitoring. A number of the prototypes are used as stand-alone devices to record ECG signals in a clinical environment, rather than as part of an integrated tele-monitoring system [12]-[13]. Meanwhile, other works have presented remote tele-monitoring systems focused on collecting ECG signals and other important biosignals, such as those related to electromyography (EMG) [14], breathing [15]-[17], accelerometery [12], [18], and galvanic skin response [13]. The systems presented in [13] also provide tools for off-line digital signal processing, gathering the principal parameters assessed from signals, including heart rate, blood pressure, respiratory rate, and activity classification.

Hexoskin (https://www.hexoskin.com/) is one of the leading e-textile based remote monitoring products that is currently commercially available. This product allows for the collection of ECG and accelerometric signals, as well as for heart and respiratory rate monitoring, heart rate variability analysis and activity intensity assessment. Here, the attendant hardware is distributed along with compatible mobile apps for real-time signal visualisation, with specific software used for basic off-line data processing.

In this manuscript, the aim is to present our prototypal system, which is based on an e-textile sensing shirt with the capacity to collect ECG, EMG and accelerometric signals. The sensing hardware uses Bluetooth low energy (BLE) technology to transmit data to a connected smartphone, enabling real-time visualisation. In exploiting the internet network, the relevant data can be shared on a dedicated server, where they can be accessed and downloaded only by authorised healthcare professionals. Raw signals can subsequently be processed using a custom-made MATLAB desktop graphical user interface (GUI) to assess a wide-ranging set of synthetic parameters. The overall aim is to provide a complete system for healthcare remote monitoring based on a textile device. Unlike many of the referenced applications, the proposed system allows for the simultaneous acquisition of ECG, EMG and acceleration signals, with their digital processing producing an extremely large set of synthetic parameters that comprehensively reflect the patient's clinical state. The innovative tool is represented by the custom-made platform that gathers a set of advanced signal-processing algorithms, collecting all the possible information from the signals. Healthcare professionals can access and manage the information in a practical way, with the possibility of directly contacting the patient through the mobile application in the case of dangerous clinical conditions.

The details of the prototype's design and development are provided in the first subsection of the following section. Meanwhile, a validation analysis of the system was also undertaken by performing comparative assessments with a standard device commonly used in clinical environments. In this work, the focus is on ECG monitoring, providing validation analysis for the raw signals collected via the prototype and for the processed data flowing from the digital signal processing. The rules followed in the validation analysis are presented in section 3, with the validation results presented in section 4. In section 5, we discuss the results, outlining the advantages, limitations and perspectives of the proposed technology. Finally, in the concluding section, the major findings are summarised.

2. MATERIALS AND METHODS

The main aim of this work was to present the novel wearable device, SWEET Shirt, for remote health monitoring, and to validate its performance in terms of the acquisition and analysis of electrocardiographic activity. In this section, we describe in detail the units that make up the novel system and the materials and methods used to perform the validation analysis.

2.1. The SWEET Shirt

The SWEET Shirt is a wearable sensing device that allows for the acquisition of electrocardiographic, bicep electromyographic and trunk acceleration signals. It can be integrated within a complete system for remote healthcare purposes, as illustrated by the schematic shown in Figure 1. The remote monitoring system includes an e-textile-based sensing sock for gait and postural assessments, as described in [19].

The wearable sensor unit allows for bio-signal acquisition when connected to the analogue front-end located in the electronic unit. This unit also contains a microcontroller and allows for data transmission through an integrated BLE module. A custom-made Android mobile application was developed to receive and visualise real-time signals on a smartphone, and to subsequently upload data on a dedicated web server. This server presents a restricted area that is exclusively accessible (following prior authentication) by authorised and appointed healthcare professionals, who can download, analyse and process the data using the custom-made MATLAB desktop software.

In the following sections, the functional modules of the system are individually presented.

2.2. Wearable sensing unit

The wearable sensing unit is comprised of a commercial elastic t-shirt in which e-textile electrodes are integrated. A knit conductive fabric with a resistance of less than 0.03 ohm per cm in any direction across the textile was used to produce the electrodes. This fabric (Adafruit Inc. www.adafruit.com – product ID: 1167) is plated with real silver, which gives it highly conductive properties. Two 4×2-cm electrodes were integrated within the garment as sensing elements for electrocardiography processes, with two 2×2-cm electrodes placed on each shirt sleeve for electromyography acquisition and a 2×2-cm electrode integrated within the upper part of the chest as a ground electrode for all the biosignals. A conductive ribbon (5 mm in width; Adafruit Inc. product ID: 1244) was then used to connect the electrodes to the output connectors of the wearable unit, represented by snap buttons placed in a pocket on the chest of the shirt. The conductive ribbon is made of woven conductive stainless-steel fibres, with a resistance of less than 0.1 ohm per cm. Conductive traces sewn onto the shirt were covered by a non-conductive fabric to avoid contact with the skin. Figure 2 shows a schematic of the wearable sensing unit, with the complete unit and the main details shown.

2.3. Electronic unit

The electronic unit is a compact module containing all the electric and electronic elements that allow for the acquisition, digitalisation and wireless transmission of the signals.

We decided to develop a custom-made analogue front-end for the ECG and EMG measurement in view of suitably dealing with the higher impedance caused by the fabric electrodes. The analogue front-end for ECG measurement comprises four principal stages: an instrumentational amplifier INA 118 from Texas Instruments, a high-pass passive filter with a cut-off frequency of 0.05 Hz, an isolation stage designed with an OpAmp LM358 in voltage follower configuration, and a low-pass active filter with a cut-off frequency of 40 Hz. The first filter is a first order high-pass CR passive filter, while the last stage is represented by a first-order active filter comprising an OpAmp LM324 in non-inverting configuration with a RC feedback.

In terms of the EMG analogue front-end, three principal stages were designed, with the first two similar to those used for the ECG analogue front-end but with the high-pass cut-off frequency set to 15 Hz. The last stage is a precision rectifier circuit with the integration of a low-pass filter. The rectifier circuit comprises an OpAmp LM324, two diodes and a resistor on the feedback connection. This form of configuration is also known as super-diode configuration. Meanwhile, a capacitor was added in parallel to the resistor to ensure this stage acts as a first-order low-pass filter. The various components were chosen to set the filter cut-off frequency at 30 Hz. The introduction of this rectifying stage was important as we are interested in the EMG envelope signal for performing the subsequent processing operations. Generally, an EMG signal is sampled and then rectified in the digital domain; however, we preferred to rectify it in the analogue domain in order to use a lower sampling frequency. The digitalisation of EMG signals requires a high sampling frequency, around 800–1,000 Hz, since the highest spectral components are at around 400–500 Hz. In contrast, an EMG envelope requires a lower sampling rate since its main spectral information is at low frequencies. The use of a lower sampling rate facilitates the real-time transmission of the signal. Moreover, using this configuration, the mobile application can provide the user with real-time EMG envelope signals, without the use of a processing stage that would increase the complexity of the system and potentially introduce delays.

The electronic board, FLORA 9-DOF (Adafruit Inc.), which mounts the triaxial inertial module iNEMO LSM9DS0, was integrated within the electronic unit to acquire accelerometric signals, while a LilyPad Simblee™ BLE board (Sparkfun Inc.), was used as the system control unit. This unit provides the digitalisation of the ECG and EMG signals and is connected to the Flora accelerometer through the serial I2C bus. The LilyPad Simblee board also allows for sending data via a BLE protocol (or Bluetooth 4.0), using the Simblee™ Bluetooth® Smart Module integrated on the shield. In fact, BLE technology presents a perfect trade-off between energy consumption, latency, piconet size, and throughput [20]. The choice of using BLE technology can also be regarded as a means of increasing the battery life of the device as much as possible. Battery life is a central issue in the development of portable devices and, in this type of application, it is mostly influenced by the data transmission operations. Indeed, BLE is one of the most data-saving transmission protocols, while other solutions have been

Figure 2. SWEET shirt sensing unit: a) internal view with textile electrodes and connections, b) external view.
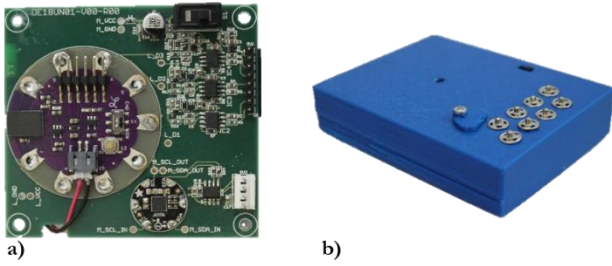
Figure 3. SWEET Shirt electronic unit: a) internal electronic unit, b) complete unit, external view.

proposed based on reducing the amount of data to be sent, using a compression method that does not degrade the signal quality [21], [22].

The control unit features were implemented through employing an ARM® Cortex M0 microcontroller that can be programmed using the Arduino IDE. The control unit was programmed to digitalise ECG and EMG analogue signals and to receive digital data from the accelerometer. Here, the ECG signal is digitalised with a sample rate of 200 Hz, while the EMG and accelerometric signals are acquired using a sample period of 15 ms (66.7 Hz). All data are collected in 20-bytes-sized packets and are sent in real time via BLE to the smartphone using the SWEET app. The packet transfer rate was set to 66.7 Hz, which was experimentally identified as the maximum rate supported by BLE transmission without data loss. Hence, each packet contains one sample from EMG and triaxial acceleration signals and three successive ECG samples in accordance with their sampling rates.

Despite the fact that the sampling rates chosen for the ECG and EMG signals were lower than those usually used, they were in line with the time resolution required by our target applications. In ECG digital processing, we are not interested in signal morphology but on heart rate analysis, which can be accurately performed with a lower sampling rate [23]. With regard to EMG signalling, the envelope signal was extracted in the analogue domain such that it can be safely sampled using the chosen rate.

All the modules that make up the electronic unit are powered by a 1,200 mAh/3.7 V lithium battery placed on the back of the unit, which is enclosed in a 3D-printed plastic case ($10 \times 7.5 \times 2$ cm³). On the top part of the case, eight snap buttons were integrated to allow for connection to the wearable sensing unit, thus providing the input signals for the analogue front ends. Figure 3 shows the internal electronic board and the complete unit.
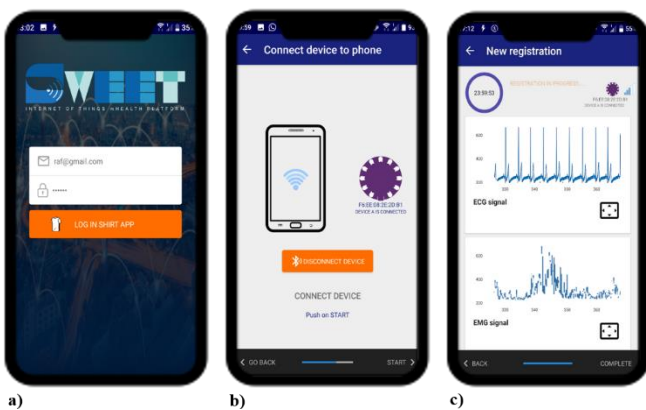
Figure 4. SWEET app main frames: a) login, b) unit connection and c) real-time signal visualisation.

2.4. The SWEET app

The SWEET app is a custom-made application for mobile devices requiring an operating system of Android 6.0 or higher and BLE technology. The application allows the smartphone to communicate and receive data coming from the electronic unit, via the BLE protocol. When the application is started, it is possible to associate and connect the wearable device using its media access control (MAC) address. Following this, the measurement session can commence, with the data transferred from the electronic unit to the mobile device, which allows for real-time signal plotting. At the end of the session, the data will be automatically saved in a '.csv' file, which is stored locally and can be uploaded at any time to a dedicated web server. Figure 4 shows the main frames of the app.

2.5. Signal processing algorithms

Data from the web server can be accessed and downloaded only by authorised healthcare professionals. The custom-made MATLAB GUI software, SWEET Lab, can be used to plot and post-process signals in order to achieve a huge set of synthetic parameters of clinical interest. In this work, we focus on ECG signal measurement and processing validation, and therefore, here, we only discuss ECG signal processing, while a number of algorithms for EMG and acceleration signal processing were developed.

The first step in ECG signal processing involves the detection of QRS complexes using an Okada algorithm [24] for the assessment of the tachogram and the discrete series of RR intervals. The subsequent analysis is divided into seven frameworks, the first of which relates to the heart rate (HR) analysis, with the instantaneous HR assessed as the mean over four successive beats. From this series, the minimum, the maximum, the medium and the median HRs can be extracted and the tachycardia ($HR > 110$ bpm) and bradycardia ($HR < 60$ bpm) events subsequently searched and listed.

The second framework is dedicated to the heart rate variability (HRV) analysis in terms of the time, frequency and

Table 1. HRV time domain variables.

Statistical Measures	
Variable	**Description**
SDNN in ms (*Standard Deviation NN-intervals*)	Standard deviation of normal-to-normal intervals (NN). SDNN reflects all cycles responsible for heart rate variation in time, thus representing the total variability.
SDANN in ms (*Standard Deviation Averaged NN-intervals*)	Standard deviation of the average NN intervals calculated over 5 min. SDNN is therefore a measure of the changes in heart rate due to cycles longer than 5 min.
SDNNi in ms (*SDNN index*)	Mean of SDs of NN intervals, calculated over 5 min.
RMSSD in ms (R*oot Mean Square of Successive Differences*)	Square root of the mean of the squares of the successive differences between adjacent NN intervals.
NN50	Number of pairs of successive NNs that differ by more than 50 ms.
pNN50 in %	Proportion of NN50 divided by total number of NN intervals.
Geometrical Measures	
Variable	**Description**
HRV Ti (*Triangular index*)	Area of the histogram distribution of RR intervals, normalised to the maximum value of the histogram.
TINN	Base width of the RR intervals histogram.

time–frequency domains. Here, the beats are first classified in terms of normal, ectopic, premature ventricular contraction (PVC) and artifacts based on their timing before the RR series is edited to exclude any artifacts and any beat-to-beat intervals that are too short or too long. The new RR series is then processed in the time domain to extract the statistical and geometrical measures, as listed in Table 1 [25].

The HRV is also assessed in the frequency domain by analysing how the power spectral density (PSD) is distributed as a function of frequency. The PSD presents three main components in terms of very low frequency (VLF), low frequency (LF) and high frequency (HF). The frequency peaks and the absolute and relative power values of each component are computed along with the LFHF ratio [26]. Three different methods are provided by the software to compute the PSD, namely, the Welch Periodogram [27], Burg Periodogram [28] and e Lomb–Scargle Periodogram [29] methods. The same analyses are conducted on the windowed periodogram of the RR series to obtain a time–frequency domain analysis of the HRV variability.

The third framework in the ECG processing relates to heart rate turbulence (HRT) analysis. This form of analysis presents a non-invasive method that explains the response of the heart to ventricular arrythmias [30] and is a good predictor of mortality following acute myocardial infarction [31]. Two numerical parameters are assessed by the software to describe HRT: turbulence onset (TO: to describe the initial acceleration in heart rate following PVC), and turbulence slope (TS: to reflect the subsequent deceleration of the sinus rhythm) [30]. Meanwhile, the fourth framework provides a nonlinear analysis of ECG signals using four different approaches: sample entropy, detrended fluctuation analysis (DFA), Poincaré plots and fractal dimension analysis (FDA). Here, sample entropy presents a nonlinear method for determining the complexity of a RR series, which is computed in terms of various values of k and is used for HRV analysis [32]. Meanwhile, DFA is used to quantify the fractal properties of brief intervals of the tachogram signal [33], while a Poincaré plot is a plot of RR intervals vs. the previous RR intervals used to quantify self-similarity. Two numerical parameters are assessed in Poincarè plot analysis: SD2 (the magnitude of the major axis of the ellipse fitting the data; represents the short-term variability) and SD1 (the magnitude of the minor axis of the ellipse; represents the long-term variability). Finally, FDA provides the measurement of the fractal dimension of the RR series assessed using a Higuchi algorithm [34]. The fractal dimension is a useful indicator in cardiology since it assumes different values for different types of heart disease [35].

3. VALIDATION ANALYSIS

Here, we present a validation analysis related to SWEET Shirt ECG signal acquisition and processing. In fact, three different type of analysis were conducted in order to address any possible unconformity in the measurement and/or processing phases managed by the new prototype. We first compared the RR
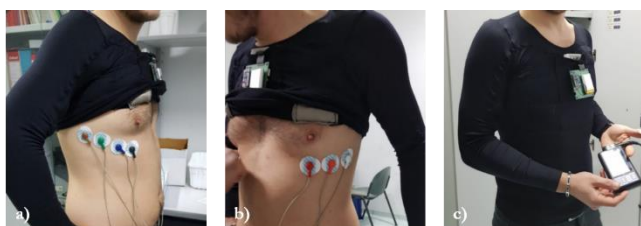
intervals identified by the SWEET Shirt with those obtained via a reference device. Following this, the similarity between the ECG signals obtained via the different devices was assessed. Finally, comparative analysis was carried out to validate a specific subset of parameters derived from the SWEET Lab software signal processing.

3.1. Experimental setup

A three-channel digital Holter recorder (Oxford Medilog FD5) was used as the reference for the ECG signal measurement. The device incorporates seven electrodes and operates with a sampling rate of 8,000 Hz and a resolution of 15.5 bits. A healthy subject, aged 25, was equipped with the clinical Holter device along with the prototypal wearable device, SWEET Shirt, for the ECG measurement (Figure 6). Here, the Holter's electrodes were placed on the subject's thorax (Figure 6a, b) in order to avoid any overlapping with the SWEET Shirt e-textile electrodes and to ensure the two ECG waveform were as similar as possible by means of visual analysis. The ECG acquisition time was set to 2 h.

3.2. Digital processing and analysis

The ECG signals from both measurement units were loaded in the MATLAB environment for pre-processing and analysis operations, with both signals passed through a notch digital filter to remove any 50 Hz interference. The R peaks in the ECG signal from the SWEET Shirt were identified using the Okada algorithm, while those in the Holter ECG were automatically detected via its own software and could be loaded in the MATLAB environment. The first analysis was carried out to compare the RR intervals by means of Passing–Bablok (PB) regression. To achieve interval-to-interval correspondence, six RR values from the Holter series were removed since they corresponded to a region of artefacts in the SWEET ECG signal. Following this, comparative analysis was performed using the MATLAB function for PB regression [36].

The waves for each beat were subsequently isolated to allow for a beat-to-beat morphology comparison. The cut-off point was chosen as the midpoint between two subsequent R peaks in order to cover the complete signal. We chose R peaks as fiducial points since no significant differences were found among the RR locations in the first analysis (see the results section). A set of a total of 6,968 corresponding beats were obtained for the analysis. The waveforms were then resampled on a normalised axis, with
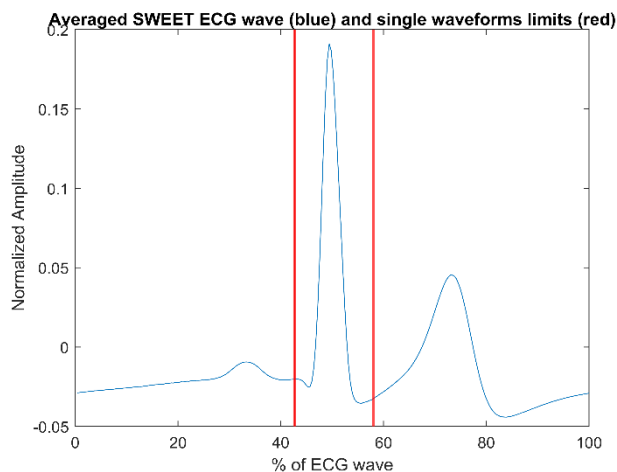
Figure 6. Average beat waveform from the SWEET Shirt and the cut-off points (red vertical lines) used to isolate single waves.

Figure 5. ECG electrode configuration used for signal acquisition.

a common number of samples in order to allow for correlation analysis among the corresponding beats. The number of samples was chosen to equal the maximum number of samples found in a non-normalised beat. A resampling operation allows for avoiding any signal distortion in the normalising time axis. We also decided to individually analyse the three principal constituent waves, namely, the P-wave, the QRS complex and the T-wave. Two cut-off points were set in the normalised time axis to divide the three single waves, which were selected to be the two stationary points between the three local maxima representing the single waves, as calculated based on the average beat waveform from the SWEET Shirt recording (Figure 5).

The complete beat and the single waveforms were rearranged in eight matrices (four for each device recording), with each column containing the signal corresponding to an occurred beat. Correlation analysis for the waveforms was carried out using the MATLAB function, 'corr', which computes the linear correlation between each pair of columns in the input matrices. The diagonal elements of the output matrix hence represent the linear correlations between the corresponding waveforms recorded by the devices under examination. The 'corr' function also returns a matrix of *p*-values for testing the hypothesis of no correlation vs. the alternative hypothesis of a non-zero correlation.

We finally compared a subset of parameters derived from our software to those provided by the commercial Holter software in order to validate our signal processing algorithms. To this end, a further 2-h ECG recording was measured using a 68-year-old volunteer experiencing a pathological disorder (cardiopathic), with the same experimental setup as used previously. The two records were then windowed in terms of 24 five-minute segments, which were individually processed, carrying out a set of 24 measures for each record and for each parameter. The ECG signals were also windowed to enlarge the dataset for the comparison, and because five minutes is the recommended duration for short-term ECG analysis [25]. Since Holter software only provides HRV measures in the time and frequency domains, validation analysis was carried out on a subset of two representative parameters, one for each HRV field, which were computed by both systems, that is, the standard deviation of normal-to-normal beats (SDNN) for the time domain, and the ratio between low- and high-frequency spectral power (LF/HF ratio) for the frequency domain. The agreement between the measures was assessed using root mean square error (RMSE), PB regression and Bland–Altman analysis.
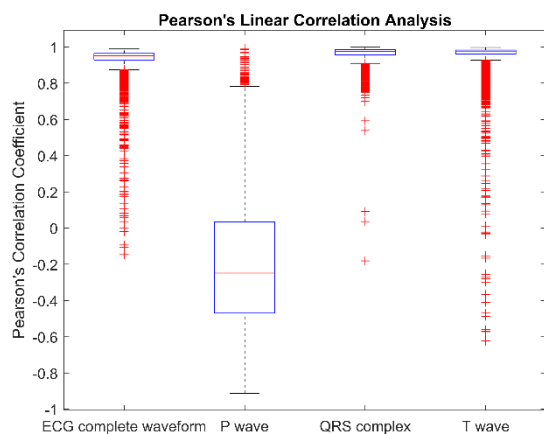
Figure 7. Boxplot of Pearson's correlation coefficient for complete and single ECG waveforms.

4. RESULTS

4.1. RR interval comparison

The RR series were compared using PB regression. This method was first proposed in 1983 as a method for testing the agreement between two sets of measurements obtained via different systems [37], [38]. Here, the PB regression involved searching for a linear relationship between the measures from the two systems and the returns slope and offset of the fitting linear model. The systems could be considered as equivalent if the confidence intervals of slope and offset contained 1 and 0, respectively. Table 2 shows the results of the PB regression for the RR intervals.

4.2. Signal waveform comparison

The ECG waveforms were compared using Pearson's linear correlation analysis. Figure 7 shows the distribution of Pearson's correlation coefficients for the complete ECG waveform, the P-wave, the QRS complex and the T-wave.

High values of correlation were found for the ECG waveform (mean value ± standard deviation: 0.94 ± 0.07), QRS complex (0.96 ± 0.04) and T-wave (0.96 ± 0.09), while lower values were returned in the P-wave analysis (-0.19 ± 0.36).

We assessed the quality of the correlation between each couple of beats using the following rules: (i) high correlation if $|r| \geq 0.7$, (ii) moderate correlation if $0.3 \leq |r| < 0.7$ and (iii) low correlation when $|r| < 0.3$. Table 3 shows a summary of the qualitative assessment of the correlation in terms of the percentage of beats, indicating high, moderate or low correlation.

Table 2. Summary statistics and results of the PB regression analysis for the RR interval series.

Statistics		Mean (StD)
RR intervals from SWEET Shirt in ms		1032 (77.44)
RR intervals from Holter MEdilog Darwin		1032 (77.41)
PB Regression	**Mean**	**Confidence interval**
Slope	1.00	1.00 to 1.00
Offset in ms	0	0 to 0

Table 3. Qualitative assessment of correlation for ECG waveforms.

	Quality of Correlation		
% of the entire set	**High**	**Moderate**	**Low**
P-wave	5.97***	49.13**	44.90
QRS complex	99.92***	0.04**	0.04
T-wave	98.87***	0.82**	0.31
ECG waveform	98.82***	0.88**	0.30

*** *p*-value < 0.001
** *p*-value < 0.005

Table 4. Main statistics and RMSE assessed for the HRV variables under examination.

	Non-Pathological Subject		
	Holter (mean ± std)	**Sweet** (mean ± std)	**RMSE**
SDNN in ms	63.2 ± 11.2	63.2 ± 11.2	0.184
LF/HF Ratio [adim]	1.54 ± 0.846	1.53 ± 0.850	0.0561
	Pathological Subject		
	Holter (mean ± std)	**Sweet** (mean ± std)	**RMSE**
SDNN in ms	20.9 ± 6,15	19.8 ± 5.87	4.41
LF/HF Ratio [adim]	3.64 ± 3,62	2.96 ± 2.92	1.97

Almost all ECG beats recorded by the prototypal device exhibited a high correlation with the corresponding waveforms obtained via the standard instrument, with a *p*-value excluding the hypothesis of null correlation between them. Specifically, the QRS complex and T-wave were the most comparable components, while the P-waves mainly exhibited moderate or low correlation values.

4.3. Signal processing algorithm validation

The first approach to the analysis of the parameters generated by the signal processing algorithms involved assessing the RMSEs among the different sets of measures. Table 4 shows the RMSE values and the principal descriptive statistics of the datasets, which were divided according to subject.

In the first section of Table 4, the results from the non-pathological volunteer session are reported. In this case, the RMSE values were extremely low for both parameters: ~0.3 % of the mean value for the SDNN and ~3.6 % of the mean value for the LF/HF ratio. However, different results were obtained with the pathological subject, with the RMSE values greater in terms of both parameters: the SDNN presented a RMSE of almost 20 % of the mean value, while the LF/HF ratio RMSE was higher than 50 % of the mean.

The analysis of agreement was then further investigated using PB regression and Bland–Altman analysis, with the attendant results presented in Table 5.

For each of the analysed parameters, the slope and offset from the PB regression are provided, along with their 95 % confidence interval (CI). Across all the results, the slope values were close to 1 and their CIs always included values of 1. Similarly, the offset values were close to 0 in all analyses, with the CIs always including 0 values. In terms of the pathological subject results, the CIs were larger than the corresponding CIs in the non-pathological subject, confirming a better agreement in the measurements derived from the recording involving the healthy volunteer.

The Bland–Altman analysis results included some bias with the 95 % CI and the limits of agreement [LoA]. In terms of the results from the non-pathological volunteer, the bias values were very close to 0, while both the bias CIs and LoA exhibited a low width and always included a 0 value. Meanwhile, in terms of the results for the pathological subject, the bias values for the SDNN and the LF/HF ratio were higher, with a wider LoA including 0.

The Bland–Altman plots are presented in Figure 8 and Figure 9. While the differences between the methods were greater in terms of both parameters assessed using the pathological subject, they exhibited a random distribution, meaning no systematic or proportional error could be confirmed from this analysis.

5. DISCUSSION

In the first analysis, we compared the RR intervals obtained via the two systems under examination by means of PB regression. The results (Table 2) confirmed that the systems can be considered as equivalent in terms of the identification of the *R* peaks along the ECG signal as beat reference points.

We then compared the signal waveforms by means of Pearson's correlation analysis. This assessment demonstrated that good agreement existed between the signals, particularly in terms of the QRS complex and T-wave, while less correspondence was found in the comparison of the P-waves (see Figure 7 and Table 3). Figure 10 shows the averaged ECG waveforms recorded by the two systems. Here, the P-waves were less visible in the Holter signal than in the SWEET Shirt
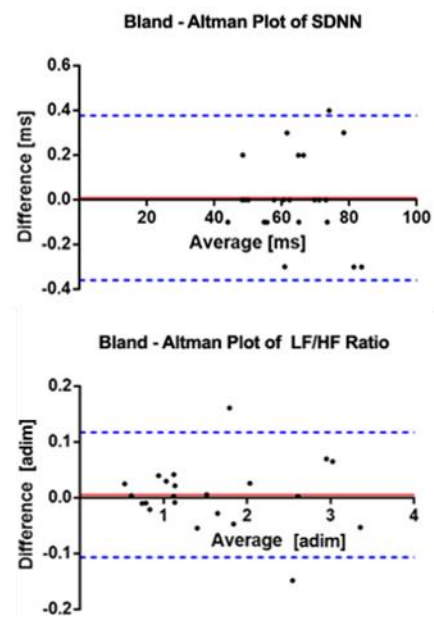
Figure 8. Bland–Altman plots of the parameters for the non-pathological volunteer. The red lines represent the bias, while the blue dashed lines represent the LoA.

recording. This was due to the non-standard electrode placement used for the Holter system (see Figure 6), which was chosen to avoid the overlapping with the textile electrodes enclosed in the shirt. Therefore, the lower agreement level with the P-waves can be attributed to the different electrode placements used, which is all but compulsory in a simultaneous recording. We can therefore affirm that the prototypal shirt has the capacity to clearly record an ECG signal that is comparable with those acquired by commonly used clinical portable devices.

Finally, we investigated the performances of the developed software in terms of signal processing. As shown in Figure 8, Table 4 and Table 5, excellent results were achieved in the analysis of the parameters assessed using the non-pathological subject. The RMSE for both parameters under examination was
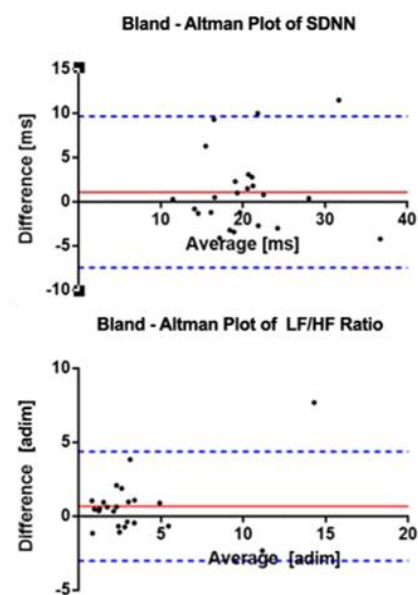
Figure 9. Bland–Altman plots of the parameters for the pathological volunteer. The red lines represent the bias, while the blue dashed lines represent the LoA.

Table 5. Results of PB regression and Bland–Altman analysis for HRV measures.

	PB Regression		Bland–Altman Analysis	
	Non-Pathological Subject			
	Slope [95 % CI]	**Offset [95 % CI]**	**Bias [95 % CI]**	**LoA**
SDNN	1.00 [0.993 to 1.01]	0 [-0.454 to 0.430]	0.00870 [-0.0713 to 0.0887]	-0.360 to 0.377
LF/HF Ratio	1.00 [0.974 to 1.04]	-0.00740 [-0.0506 to 0.0273]	0.00539 [-0.0189 to 0.0297]	-0.107 to 0.117
	Pathological Subject			
	Slope [95 % CI]	**Offset [95 % CI]**	**Bias [95 % CI]**	**LoA**
SDNN	0.932 [0.597 to 1.39]	0.692 [-8.86 to 7.02]	1.10 [-0.711 to 2.92]	-7.44 to 9.65
LF/HF Ratio	0.919 [0.618 to 1.39]	-0.409 [-1.50 to 0.358]	0.684 [-0.101 to 1.47]	-3.01 to 4.38

extremely low, as were the biases assessed via the Bland–Altman analysis. Meanwhile, the PB analysis revealed that there was a regression line very close to the identity line, underlining a strict correspondence between the measurements from the two devices. However, lower agreement was found in the analysis involving the pathological subject. Here, the RMSE and bias values were higher (Table 4) and the PB CIs were wider (Table 5), albeit that they still involved values that allowed for concluding that there was some agreement between the two methods. However, the Bland–Altman plots (see Figure 9) did not exhibit any prevalent trend in the distribution of the differences, thus suggesting that no systematic or proportional differences existed between the measurement systems.

Based on these results, the lower agreement level in the parameters related to the pathological subject can be attributed to the greater presence of artefacts in the SWEET Shirt record, which was likely due to the weak adherence of the textile electrodes on the patient's skin or the higher number of movements made by the subject during the recording session. The ECG signal from the SWEET Shirt was clearly visible in 94.66 % of the registration time, while the signal from the Holter recorder did not present any artefacts. The presence of artefact regions will affect any signal processing results since the artefacts must be replaced by a specific number of normative RR intervals to ensure the continuity of the RR series. In this case, the results were further affected by the fact that they were averaged using a reduced window of 5 min.

6. CONCLUSIONS

In this paper, a new textile-sensor-based wearable device for the measurement and analysis of vital signals was developed and presented. The innovative features of the system rely on the multi-parametric approach in health monitoring and on the wide-ranging set of tools available for digital signal processing. In the development of the sensing unit, various sensors, electrodes, and bus structures were integrated within the textile garment, making it possible for the patient to perform normal daily activities without any discomfort while their clinical status is monitored by a specialist. The system includes a custom-based app for real-time visualisation of the acquired signals and a software desktop for off-line plotting and digital signal processing.

In this work, we described the design of the device and provided a validation analysis related to ECG measurement and digital processing. Here, encouraging results were achieved, indicating that reliable measurements can be obtained using our prototype wearable device, both in terms of ECG signal acquisition and further signal processing. In terms of possible improvements, the adherence of the electrodes must be increased to reduce motion artifacts interfering with the signal, which is, in our experience, the major issue encountered in this area, one that can seriously affect processing operations.

Figure 10. Comparison of averaged ECG beat waveforms from the Holter device (blue) and the sensorised shirt (red).

REFERENCES

[1] J. P. DiMarco, J. T. Philbrick, Use of ambulatory electrocardiographic (Holter) monitoring, Annals of Internal Medicine, 113(1) (1990), pp. 53-68.
DOI: 10.7326/0003-4819-113-1-53

[2] P. Verdecchia, C. Porcellati, G. Schillaci, C. Borgioni, A. Ciucci, M. Battistelli, M. Guerrieri, C. Gatteschi, I. Zampi, A. Santucci, C. Santucci, G. Reboldi, Ambulatory blood pressure. An independent predictor of prognosis in essential hypertension, Hypertension 24(6) (1994), pp. 793-801.
DOI: 10.1161/01.hyp.24.6.793

[3] J. A. Gjevre, R. M. Taylor-Gjevre, R. Skomro, J. Reid, M. Fenton, D. Cotton, Comparison of polysomnographic and portable home monitoring assessments of obstructive sleep apnea in Saskatchewan women, Canadian Respiratory Journal 18 (2011), pp. 271-274.
DOI: 10.1155/2011/408091

[4] T. Pawar, S. Chaudhuri, S. P. Duttagupta, Body movement activity recognition for ambulatory cardiac monitoring, IEEE Transactions on Biomed. Engin. 54(5) (2007), pp. 874-882.
DOI: 10.1109/TBME.2006.889186

[5] A. Coccia, B. Lanzillo, L. Donisi, F. Amitrano, G. Cesarelli, G. D'Addio, Repeatability of spatio-temporal gait measurements in parkinson's disease, Proc. of IEEE Medical Measurements and

Applications, MeMeA, Bari, Italy, 2020, 6 pp.
DOI: 10.1109/MeMeA49120.2020.9137357

[6] L. Donisi, A. Coccia, F. Amitrano, L. Mercogliano, G. Cesarelli, G. D'Addio, Backpack influence on kinematic parameters related to timed up and go (TUG) test in school children, Proc. of IEEE Medical Measurements and Applications, MeMeA, Bari, Italy, 2020, 5 pp.
DOI: 10.1109/MeMeA49120.2020.9137198

[7] S. Park, S. Jayaraman, The wearables revolution and Big Data: the textile lineage, The Journal of The Textile Institute 108(4) (2017), pp. 605-614.
DOI: 10.1080/00405000.2016.1176632

[8] C. Erdmier, J. Hatcher, M. Lee, Wearable device implications in the healthcare industry, Journal of Medical Engineering & Technology 40(4) (2016), pp. 141-148.
DOI: 10.3109/03091902.2016.1153738

[9] H. Lewy, Wearable technologies–future challenges for implementation in healthcare services, Healthcare Technology Letters 2(1) (2015), pp. 2-5.
DOI: 10.1049/htl.2014.0104

[10] A. Pantelopoulos, N. G. Bourbakis, A survey on wearable sensor-based systems for health monitoring and prognosis, IEEE Transactions on Systems, Man, and Cybernetics, Part C (Applications and Reviews) 40(1) (2009), pp. 1-12.
DOI: 10.1109/TSMCC.2009.2032660

[11] D. Pani, A. Achilli, A. Bonfiglio, Survey on textile electrode technologies for electrocardiographic (ECG) monitoring, from metal wires to polymers, Advanced Materials Technologies 3(10) (2018), 1800008.
DOI: 10.1002/admt.201800008

[12] M. Di Rienzo, F. Rizzo, G. Parati, G. Brambilla, M. Ferratini, P. Castiglioni, MagIC system: a new textile-based wearable device for biological signal monitoring applicability in daily life and clinical setting, Proc. 27th Ann. Int. IEEE EMBS Conf., Shanghai, China, 1 – 4 September 2005, pp. 7167-7169
DOI: 10.1109/IEMBS.2005.1616161

[13] P. S. Pandian, K. Mohanavelu, K. P. Safeer, T. M. Kotresh, D. T. Shakunthala, P. Gopal, V. C. Padaki, Smart vest: Wearable multiparameter remote physiological monitoring system, Med. Eng. Phys. 30 (2008), pp. 466-477.
DOI: 10.1016/j.medengphy.2007.05.014

[14] R. Paradiso, G. Loriga, N. Taccini, A wearable health care system based on knitted integral sensors, IEEE Trans. Inf. Technol. Biomed. 9(3) (2005), pp. 337-344.
DOI: 10.1109/titb.2005.854512

[15] S. Coyle, K.-T. Lau, N. Moyna, D. O'Gorman, D. Diamond, F. Di Francesco, D. Costanzo, P. Salvo, M. Giovanna Trivella, D. Emilio De Rossi, N. Taccini, R. Paradiso, J.-A. Porchet, A. Ridolfi, J. Luprano, C. Chuzel, Th. Lanier, F. Revol-Cavalier, S. Schoumacker, V. Mourier, I. Chartier, R. Convert, H. De-Moncuit, C. Bini, BIOTEX—Biosensing textiles for personalised healthcare management, IEEE Transactions on Information Technology in Biomedicine 14(2) (2010), pp. 364-370.
DOI: 10.1109/TITB.2009.2038484

[16] J. De jonckheere, M. Jeanne, A. Grillet, S. Weber, P. Chaud, R. Logier, J. L. Weber, OFSETH: Optical fibre embedded into technical textile for healthcare, an efficient way to monitor patient under magnetic resonance imaging, Proc. of 29th IEEE Annual International Conference of the IEEE Engineering in Medicine and Biology Society, Lyon, France, 22-26 August 2007, pp. 3950-3953.
DOI: 10.1109/iembs.2007.4353198

[17] J. P. S. Cunha, B. Cunha, A. S. Pereira, W. Xavier, N. Ferreira, L. Meireles. Vital-Jacket®: a wearable wireless vital signs monitor for patients' mobility in cardiology and sports, 4th IEEE International Conference on Pervasive Computing Technologies for Healthcare, Munchen, Germany, 22–25 March 2010, pp. 1-2.
DOI: 10.4108/ICST.PERVASIVEHEALTH2010.8991

[18] J. Luprano, J. Solà, S. Dasen, J. M. Koller, O. Chételat, Combination of body sensor networks and on-body signal processing algorithms: the practical case of MyHeart project, Proc. IEEE International Workshop on Wearable and Implantable Body Sensor Networks, Cambridge, Massachusetts, USA, 3 – 5 April 2006, p. 4.
DOI: 10.1109/BSN.2006.15

[19] F. Amitrano, L. Donisi, A. Coccia, A., Biancardi, G. Pagano, G. D'Addio, Experimental development and validation of an E-textile sock prototype, Proc. of IEEE Medical Measurements and Applications MeMeA, Bari, Italy, 2020.
DOI: 10.1109/MeMeA49120.2020.9137302

[20] C. Gomez, J. Oller Bosch, J. Paradells, Overview and evaluation of Bluetooth low energy: an emerging low power wireless technology, Sensors 12 (2012), pp. 11734-53.
DOI: 10.3390/s120911734

[21] E. Balestrieri, P. Daponte, L. De Vito, F. Picariello, S. Rapuano, I. Tudosa, A Wi-Fi IoT prototype for ECG monitoring exploiting a novel compressed sensing method, Acta IMEKO 9 (2020) 2, pp. 38-45.
DOI: 10.21014/acta_imeko.v9i2.787

[22] F. Picariello, G. Iadarola, E. Balestrieri, I. Tudosa, L. De Vito, A novel compressive sampling method for ECG wearable measurement systems, Measurement 167 (2021).
DOI: 10.1016/j.measurement.2020.108259

[23] S. Mahdiani, V. Jeyhani, M. Peltokangas, A. Vehkaoja, Is 50 Hz high enough ECG sampling frequency for accurate HRV analysis? 37th Annual International Conference of the IEEE Engineering in Medicine and Biology Society (EMBC), Milan, Italy, 25–29 August 2015, pp. 5948-5951.
DOI: 10.1109/EMBC.2015.7319746

[24] M. Okada, A digital filter for the QRS complex detection. IEEE Transactions on Biomedical Engineering (12) (1979), pp. 700-703.
DOI: 10.1109/TBME.1979.326461

[25] Task Force of the European Society of Cardiology, Heart rate variability: standards of measurement, physiological interpretation and clinical use, Circulation 93 (1996), pp. 1043-1065.
DOI: 10.1161/01.CIR.93.5.1043

[26] A. Malliani, M. Pagani, F. Lombardi, S. Cerutti, Cardiovascular neural regulation explored in the frequency domain, Circulation 84 (1991), pp. 482-492.
DOI: 10.1161/01.cir.84.2.482

[27] P. Welch, The use of fast Fourier transform for the estimation of power spectra: a method based on time averaging over short, modified periodograms, IEEE Transactions on Audio and Electroacoustics 15(2) (1967), pp. 70-73.
DOI: 10.1109/TAU.1967.1161901

[28] J. P. Burg, Absolute power density spectra, In Maximum-Entropy and Bayesian Methods, in: Inverse Problems. Springer, Dordrecht, 1985, ISBN 978-90-481-8418-7, pp. 273-286.

[29] N. R. Lomb, Least-squares frequency analysis of unequally spaced data. Astrophysics and Space Science 39(2) (1976), pp. 447-462.
DOI: 10.1007/BF00648343

[30] I. Cygankiewicz, W. Zaręba, Heart rate turbulence-an overview of methods and applications, Cardiology Journal 13(5) (2006), pp. 359-368.

[31] G. Schmidt, M. Malik, P. Barthel, R. Schneider, K. Ulm, L. Rolnitzky, A. J. Camm, J. T. Bigger Jr., A. Schömig, Heart-rate turbulence after ventricular premature beats as a predictor of mortality after acute myocardial infarction, The Lancet, 353(9162) (1999), pp. 1390-1396.
DOI: 10.1016/S0140-6736(98)08428-1

[32] H. M. Al-Angari, A. V. Sahakian, Use of sample entropy approach to study heart rate variability in obstructive sleep apnea syndrome, IEEE Transactions on Biomedical Engineering 54(10) (2007), pp. 1900-1904.
DOI: 10.1109/TBME.2006.889772

[33] H. V. Huikuri, T. H. Makikalli, C. K. Peng, A. L. Goldberger, U. Hintze, M. Moller, Fractal correlation properties of R–R interval dynamics and mortality in patients with depressed left ventricular function after an acute myocardial infarction, Circulation 101

(2000), pp. 47-53.
DOI: 10.1161/01.cir.101.1.47

[34] T. Higuchi, Approach to an irregular time series on the basis of the fractal theory, Physica D (1998), pp. 277-283.
DOI: 10.1016/0167-2789(88)90081-4

[35] R. Acharya, P. S. Bhat, N. Kannathal, A. Rao, C. M. Lim, Analysis of cardiac health using fractal dimension and wavelet transformation, ITBM-RBM 26(2) (2005), pp. 133-139.

[36] A. Padoan (2020). Passing and Bablok regression, MATLAB Central File Exchange. Online [Accessed 24 June 2020]
https://www.mathworks.com/matlabcentral/fileexchange/24894-passing-and-bablok-regression

[37] H. Passing, W. Bablok, A new biometrical procedure for testing the equality of measurements from two different analytical methods. Application of linear regression procedures for method comparison studies in clinical chemistry, Part I. Clinical Chemistry and Laboratory Medicine 21(11) (1983), pp. 709-720.
DOI: 10.1515/cclm.1983.21.11.709

[38] W. Bablok, H. Passing, Application of statistical procedures in analytical instrument testing, Journal of Analytical Methods in Chemistry 7(2) (1985), pp. 74-79.
DOI: 10.1155/S1463924685000177